

Compressive Spectrum Sensing Front-ends for Cognitive Radios

(Invited Paper)

Zhuizhuan Yu, Sebastian Hoyos
Analog and Mixed Signal Center, ECE Department
Texas A&M University
College Station, TX, 77843-3128
Email: zyu@neo.tamu.edu, hoyos@ece.tamu.edu

Abstract—We propose a novel parallel mixed-signal compressive spectrum sensing architecture for Cognitive Radios (CRs) with a detailed study of the signal modeling. The mixed-signal compressive sensing is realized with a parallel segmented compressive sensing (PSCS) architecture, which not only can filter out all the harmonic spurs that leak from the local random generator, but also provides a tradeoff between the sampling rate and the system complexity such that a practical hardware implementation is possible. We consider application of the architecture to do spectrum estimation, which is the first step for spectrum sensing in CRs. The benefit of prior knowledge about the input signal's structure is explored and it is shown that this can be exploited in the PSCS architecture to greatly reduce the sampling rate.

Index Terms—Compressive sensing, mixed-signal, spectrum sensing, cognitive radio, compact signal modeling

I. INTRODUCTION

Cognitive Radios (CRs), first proposed in [1], provides a revolutionary paradigm to improve the frequency usage efficiency by allowing Dynamic Spectrum Access (DSA). In CRs, *spectrum holes* that are unoccupied by primary users can be assigned to appropriate secondary users as long as the interference introduced by secondary users is not harmful to primary users [2]–[4]. The design of cognitive radio networks is a complicated cross-layer procedure [5]. In this paper, we focus on the *spectrum sensing* problem in CRs, that is, to sense (detect) the existence of primary users, since this is the first task for CRs in order to realize the DSA.

Spectrum sensing can be a very challenging task for CRs due to many factors. First, for the sake of improving the frequency usage efficiency, the sensing bandwidth for CRs can expand from hundreds of MHz to several GHz. Second, the sensing radio should be able to detect very weak primary users, known as *hidden terminals* [5]. With the traditional time-domain Nyquist sampling, it is usually power-hungry to digitize signals with both wide bandwidth and high dynamic range. For example, suppose the sensing radio should detect a weak signal of $1\mu V$ from a $100mV$ interferer. These observed signal levels are not uncommon in a typical fading wireless environment, and result in the need for 16-bit ADC resolution. Achieving this over a large bandwidth of 5GHz say, the required power consumption of this ADC would be 1kW [6] under a rather optimistic assumption on the energy consumption at 1 pJ per conversion [7]. Obviously, trying to

achieve the wideband spectrum sensing for CRs by brute-forcefully implementing the high-speed and high-resolution ADC is not realistic with current technologies. An alternative for the RF front-end is to use a bank of filters each of which senses a certain range of narrow bandwidth. However, this imposes strict constraints on the filter design.

Fortunately, today's spectrum usage presents some *sparsity* in the sense that only a small portion of frequency bands are heavily loaded while others are partially or rarely occupied at certain time and certain place. This frequency usage sparsity can be utilized under the framework of Compressed Sensing (CS) [8], [9] to reduce the sensing rate at the sensing radio of CRs. According to CS theories, the characteristics of a signal that is sparse over some signal basis can be completely captured by a number of projections over another basis which is incoherent with the signal basis and then reconstructed perfectly from these random projections at a high probability. The number of random projections is on the order of the signal's information rate rather than the Nyquist rate.

This idea of applying CS to do wideband spectrum sensing was first introduced in [10]. However, this approach assumes perfect analog-to-digital conversion and the issue is to reduce the complexity of the spectrum estimate. As a result, a full-rate sampling is still required, which is just the most challenging task. A mixed-signal parallel segmented compressive sensing (PSCS) architecture to do wideband spectrum sensing in CRs was proposed in [11], where the high-speed ADCs were avoided by applying the CS to the analog signal directly.

In this paper we further develop and study the PSCS architecture [11] and its application on wideband spectrum sensing for CRs. The remainder of this paper is organized as follows. A brief background on CS is provided in section II and the spectral occupancy signal modeling is given in section III. Section IV introduces the proposed mixed-signal parallel compressive spectrum sensing scheme. Section V discusses how prior knowledge can be utilized via the *compact* signal modeling to reduce the sampling rate. Conclusions are made in section VI.

II. COMPRESSIVE SENSING BACKGROUND

Given a vector of discrete-time signal samples $\mathbf{r}_{P \times 1}$ that is *K-sparse* or *compressible* in some basis matrix $\Psi_{P \times S}$,

i.e. $\mathbf{r} = \Psi \mathbf{a}$, where $\mathbf{a}_{S \times 1}$ has only K non-zero elements, we can reconstruct the signal successfully with high probability from L measurements, where L depends on the reconstruction algorithm and is usually much less than P .

In CS, the *measurement* is done by projecting \mathbf{r} over another random basis Φ that is incoherent with Ψ , i.e. $\mathbf{y} = \Phi \Psi \mathbf{a}$. The *reconstruction* is performed by solving the following l_1 -norm optimization problem.

$$\hat{\mathbf{a}} = \arg \min \|\mathbf{a}\|_1 \quad s.t. \mathbf{y} = \Phi \Psi \mathbf{a} = V \mathbf{a}, \quad (1)$$

for which linear programming (LP) techniques or iterative greedy algorithms such as orthogonal matching pursuit (OMP) can be used. When LP is used to do the reconstruction, M is approximately $O(K \log(S/K))$ to achieve a reasonable reconstruction quality.

In practice the measurements are inevitably polluted by noise. Assuming the noise is additive, i.e., $\mathbf{r} = \Psi \mathbf{a} + \mathbf{n}$, then the reconstruction can be formulated as the following SOCP (second order cone programming) problem,

$$\hat{\mathbf{a}} = \arg \min \|\mathbf{a}\|_1 \quad s.t. \|\mathbf{y} - \Phi \Psi \mathbf{a}\|_2 \leq \epsilon, \quad (2)$$

where $\epsilon = \|\Phi \mathbf{n}\|_2$.

III. SIGNAL MODELING

The input signal to the sensing radio $r(t)$ is a multi-band analog signal whose spectrum is illustrated in Fig.1. Specifically, we assume that $r(t)$, with a frequency span from f_l to f_h , is the superposition of primary users, perhaps using W different wireless standards [5]. Each wireless standard occupies a certain frequency band which consists of multiple channels. According to the measurements done by FCC in the US [12], the current frequency usage exhibits sparsity because only a part of the allocated channels for one standard are utilized at a given time.

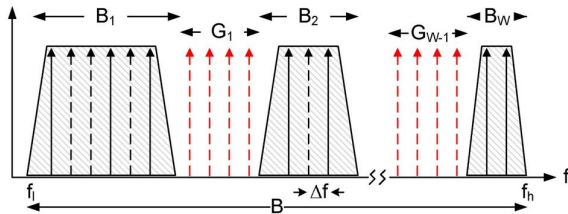


Fig. 1. Illustration of the multi-band analog signal to the sensing radio.

Without loss of generality, we assume that $r(t)$ is bandlimited to $[0, f_h]$, so $r(t)$ can be written as

$$r(t) = \int_{-\infty}^{\infty} R(f) e^{j2\pi f t} df = \int_0^{f_h} R(f) e^{j2\pi f t} df, \quad (3)$$

where, $R(f)$ is the Fourier transform of $r(t)$. The spectrum hole detection such as energy detection and feature detection is usually based on the observation of $R(f)$. In practice, we are interested in regimes where it is not realistic to have continuous observation of $R(f)$, therefore, $r(t)$ is approximated as

$$r(t) \approx \sum_{s=0}^{S-1} R(s\Delta f) e^{j2\pi s\Delta f t} \Delta f, \quad (4)$$

where Δf is the resolution on the frequency axis and $(S-1)\Delta f = f_h$. In other words, $r(t)$ is approximated as a multi-carrier signal bandlimited to $[0, f_h]$ and with a carrier spacing of Δf . The sparsity on frequency usages means that statistically speaking, only K out of the S carriers are active at any time, where $K \ll S$. This model is convenient for representing user occupancy with spectral sparsity.

Assuming the channel state information is known at the receiver and the noise is additive Gaussian bandlimited to $[0, f_h]$, we can then employ a *direct modeling* of the input signal as:

$$r(t) = \sum_{s=0}^{S-1} a_s \Psi_s(t) + n(t), \quad (5)$$

where $n(t)$ is AWGN noise, $\Psi = [\Psi_0(t), \Psi_1(t), \dots, \Psi_{S-1}(t)]$, $\Psi_s(t) = e^{j2\pi s\Delta f t}$, $\mathbf{a} = [a_0(t), a_1(t), \dots, a_{S-1}(t)] \in \mathbb{C}^S$, $a_s = \Delta f R(s\Delta f)$ and \mathbf{a} has only $K \ll S$ non-zero elements. Since Δf is a scalar, for simplicity, we discard it in the following and model the input signal as a multi-carrier signal with $a_s = R(s\Delta f)$.

Note that these W frequency bands are not necessarily consecutive. Between two neighboring frequency bands, there may exist some frequency *gaps* which are not allowed for use or the information over which is not useful to the receiver and therefore can be filtered out. If we know the location of the frequency *gaps*, we can have a *compact modeling* of $r(t)$ as:

$$r(t) = \sum_{s'=0}^{S'-1} a_{s'} \Psi_{s'}(t) + n(t), \quad (6)$$

where, s' is a non-consecutive enumeration of those carriers within the W frequency bands. For example, if we index the S carriers from f_l to f_h by $1, 2, \dots, i-1, i, \dots, j, j+1, \dots, S$, and the carriers indexed from i to j are within the frequency *gap*, then the compact signal model only includes the carriers indexed by $1, 2, \dots, i-1, j+1, \dots, S$ and $S' = S - (j - i + 1)$. This compact modeling is crucial for reducing the sampling rate via the a priori knowledge of the frequency gap locations.

Based on Fig. 1, we define the following parameters.

◆ **NBW** The nominal bandwidth of the input signal to the receiver.

$$NBW = f_h - f_l = \sum_{i=1}^W B_i + \sum_{i=1}^{W-1} G_i.$$

◆ **EBW** The effective accessible bandwidth of the receiver.

$$EBW = \sum_{i=1}^W B_i.$$

◆ **OBW** The actual occupied bandwidth of the input signal to the receiver.

◆ **NSP** The nominal sparsity of the input signal, which is the occupied bandwidth over the NBW

$$NSP = \frac{OBW}{NBW}.$$

- ◇ **ESP** The effective sparsity of the input signal, which is the occupied bandwidth over the EBW,

$$ESP = \frac{OBW}{EBW}.$$

- ◇ **FNq** The required Nyquist sampling rate.

$$F_{Nq} = 2 * NBW.$$

Note that in this paper, when we talk about the Nyquist sampling rate, we always assume that the signal is downconverted to baseband before the sampling and therefore $F_{Nq} = 2 * NBW = 2 * (f_h - f_l) \neq 2 * f_h$.

- ◇ **Fcs** The overall required sampling rate for the PSCS architecture, which varies with different post-processing and reconstruction algorithms. The sampling rate at each path is approximately $1/N$ of F_{CS} .
- ◇ **NSR** The PSCS sampling rate normalized by the Nyquist sampling rate.

$$NSR = \frac{F_{CS}}{F_{Nq}}.$$

Using the multi-carrier signal model with a carrier spacing of Δf , we have

$$K = \frac{OBW}{\Delta f}, \quad S = \frac{NBW}{\Delta f}, \quad S' = \frac{EBW}{\Delta f} \quad (7)$$

and

$$NSP = \frac{K}{S}, \quad ESP = \frac{K}{S'}. \quad (8)$$

IV. WIDEBAND PARALLEL COMPRESSIVE SPECTRUM SENSING

Wideband spectrum sensing is composed of several crucial steps: first, spectrum estimation; second, calculate the sufficient statistics, during which digital signal processing is needed to improve the front-end sensing sensitivity by processing gain and identification of the primary users based on knowledge of the signal characteristics [5]; last, to decide whether there exist primary users based on the sufficient statistics. Here we focus on the wideband spectrum estimation step, that is, to estimate the unknown coefficients \mathbf{a} in the equation (5) or (6). Specifically, the signal will be sampled at sub-Nyquist rate by the mixed-signal architecture given in section IV-A and the spectrum estimation will be done as shown in section IV-B.

A. Mixed-signal Compressive Sensing Architecture

The proposed *parallel segmented compressive sensing (PSCS)* structure is shown in Fig. 2. The received signal $r(t)$ for $t \in [0, T]$ is segmented into M pieces $r_m(t) = r(t)w_m(t)|_{m=0}^{M-1}$ with a duration time T_c , where, $T = 1/\Delta f = \frac{2S}{f_{Nq}}$, and $w_m(t)$ is the windowing function. Two adjacent segments can have an overlapping time $T_c - T_m$ which defines an overlapping percentage $OVR = \frac{T_c - T_m}{T_c}$, as shown in Fig. 3. Random projection is applied to each segment independently through N parallel branches. There are a total of $L = MN$

samples generated every T seconds and the m_{th} measurement of the n_{th} branch is given by

$$y_{mN+n} = \langle r_m(t), \Phi_{mN+n}(t) \rangle = \int_{mT_m}^{mT_m+T_c} r(t) \Phi_{mN+n}^*(t) dt, \quad (9)$$

where, $\Phi_{mN+n}(t)$ is chosen randomly for all m and n . At the end of each integration time T_c , the outputs of the integrators are fed to a set of ADCs and the quantized digital words are sent to the DSP blocks for further processing.

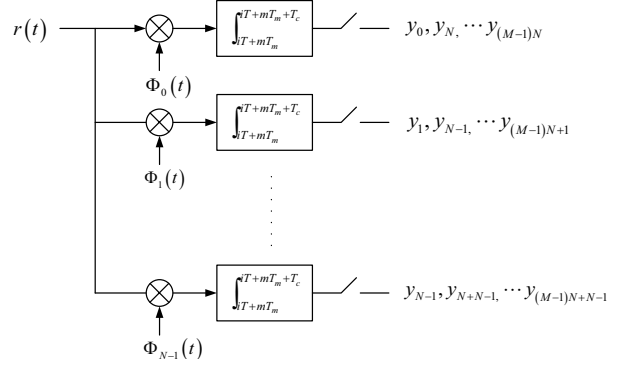


Fig. 2. Block diagram of the parallel segmented compressive sensing (PSCS) architecture.

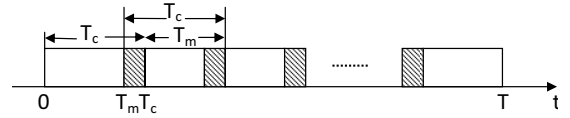


Fig. 3. Illustration of overlapping windows

The windowed integrator with overlapping acts as a spurious frequency rejection mechanism in the PSCS architecture. The integrator, with a reset every T_c seconds, provides a simple realization of a sinc type low-pass filter with nulls at frequencies of $1/T_c \times k$. By setting the random generator clock frequency equal to a harmonic of the reset frequency, the sinc nulls coincide with spur frequencies from the random generator clock and so filters them. Note also that the overlap in the integration windows provides wider filter nulls which improves the harmonic rejection. Fig. 4 compares the mean square error (MSE) of a reconstructed signal under a noiseless channel using windowed integrators parameterized by several overlapping ratios. We used a multi-carrier signal as defined in equation (5) with $S = 128$, and $K = 10$. M is fixed to be 16, which means that the sampling rate for each path is $\frac{1}{32} F_{Nq}$. An interference of -10dB relative to the single carrier's power is added after the mixer at $0.75 F_{Nq}$, that is, 24 times the single path's sampling rate. As shown in the figure, by increasing the overlapping ratio we get better reconstruction quality which is attributed to the larger attenuation on the interference.

For the random basis $\Phi_l(t)$ there are several choices, such as Gaussian, Bernoulli and so on. Here, the Bernoulli random basis has particular merit because the desired binary waveforms can be generated with digital sequential circuits.

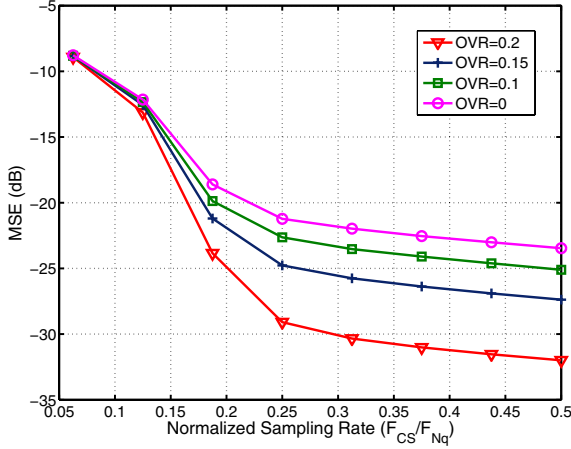


Fig. 4. The MSE of the reconstructed signal parameterized by several windowed integrators overlapping ratios.

In the PSCS architecture, the Nyquist rate ADC is avoided with the mixed-signal approach, and the sub-Nyquist sampling is achieved with the aid of CS and parallelization. First, the signal sparsity is utilized by CS to reduce the sampling rate. Depending on the application and reconstruction algorithm, the achievable sampling rate reduction varies. The parallelization reduces the sampling rate needed per path, and provides a trade-off between the sampling rate at each path and the system complexity. When $N = 1$, the architecture is equivalent to a single path architecture [13]. At the other extreme, when $M = 1$, each parallel branch generates only 1 sample per T sec, that is, the sampling rate at each branch is $f_{Nq}/2S$. The parallel architecture enables a balance to be set, avoiding too many branches and the associated hardware complexity, while tuning the associated sampling rates per branch. In addition, the output digital data is well matched to further high speed parallel digital processing. Interested readers are referred to [11] for detailed discussion.

B. Subsequent DSP

After obtaining the $L = MN$ compressed samples, these samples are concatenated to form a measurement vector given by

$$\mathbf{y} = [\tilde{\mathbf{y}}_0^T, \tilde{\mathbf{y}}_1^T, \dots, \tilde{\mathbf{y}}_{M-1}^T]^T, \quad (10)$$

where, $\tilde{\mathbf{y}}_m = [y_{mN}, y_{mN+1}, \dots, y_{mN+N-1}]^T$ is the vector of measurements from the m th segment from all N branches. Define the reconstruction matrix $V = \{v_{i,j}\}_{L \times S}$ with

$$V_{mN+n,s} = \langle \Psi_{s,m}(t), \Phi_{mN+n}(t) \rangle = \int_0^T \Psi_{s,m}(t) \Phi_{mN+n}^*(t) dt, \quad (11)$$

where, $\Psi_{s,m}(t) = \Psi_s(t)w_m(t)$.

Using \mathbf{y} and V , we can estimate $\hat{\mathbf{a}}$ by solving the optimization problem given in (2), for which there are many algorithms to choose such as SOCP, OMP, or BP (belief propagation).

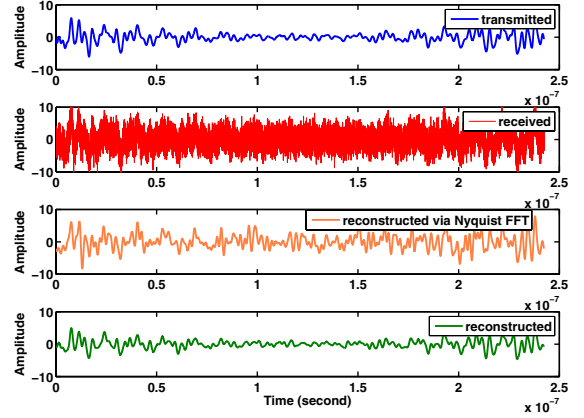


Fig. 5. Time-domain signals of a simulated multi-band signal. From top to bottom, the four plots represent the transmitted signal by primary users, the received primary users' signal at the sensing radio, the reconstructed signal from the time-domain samples via the Nyquist rate ADC and the reconstructed signal from the transform-domain samples via mixed-CS at a NSR of 0.32.

C. A Wideband Spectrum Sensing Example

In this part, we carried our a simulation to show the effectiveness of the proposed wideband PSCS architecture, where the input signal is modeled as a frequency-domain sparse multi-carrier signal as given in Equation (5). The mixed-signal compressive sensing based on the PSCS architecture given in Fig. 2 is used to do the spectrum estimation.

In the simulation, $S = 128$, $K = 17$ and $SNR_{overall} = -10$ dB, where $SNR_{overall}$ is the total signal power over the whole NBW divided by the total noise power over the NBW . Note how noisy the received signal is in this example, Fig. 5). There are 5 primary bands with $NBW=528$ MHz. Using $\Delta f = 4.125$ MHz, the primary user's frequencies are [17, 18, 43, 44, 45, 63, 64, 65, 66, 67, 76, 77, 118, 119, 120, 121, 122] $\times 4.125$ MHz. The input power dynamic range of the primary users is 15dB, and no *a priori* knowledge is assumed available at the sensing radio. In Figs. 5 and 6, from top to bottom, the four plots represent the transmitted signal by the primary users, the received primary users' signal at the sensing radio, the reconstructed signal from the time-domain samples via the Nyquist rate ADC, and the reconstructed signal from the transform-domain samples via mixed-CS at a NSR of 0.32. The measured MSE for the two reconstructed signals is -5 dB and -14dB, respectively. Note that even with a lower sampling rate, the sensing radio based on mixed-signal PSCS is more robust against noise than the traditional digital approach based on the DFT, because CS takes advantage of the knowledge of the signal structure and its sparsity.

V. SAMPLING RATE REDUCTION FROM SIGNAL MODELING

While the mixed-signal PSCS architecture can achieve wideband spectrum sensing at sub-Nyquist rate, the sampling rate reduction is limited because the number of samples needed for successful reconstruction is about four times the number of non-zero signal samples [14], which implies that signals

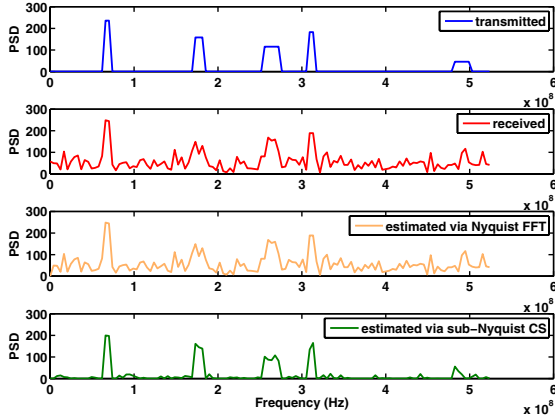


Fig. 6. Frequency-domain signals of a simulated multi-band signal. From top to bottom, the four plots represent the transmitted signal by primary users, the received primary users' signal at the sensing radio, the reconstructed signal from the time-domain samples via the Nyquist rate ADC and the reconstructed signal from the transform-domain samples via mixed-CS at a NSR of 0.32.

with sparsity larger than 25% would provide no sampling reduction in comparison with Nyquist sampling. In this section, we will investigate the potentials for sampling rate reduction from signal modeling.

Recall that we define two signal modeling schemes, *direct modeling* and *compact modeling* in section III. In the following context, we do a comparison between these two schemes in terms of the sampling rate reduction to see the benefit of a priori knowledge about the spectral gaps. Not considering the noise and using LP for reconstruction, we can estimate the required sampling rate of both schemes as follows [15].

Direct Modeling: The number of samples needed during $T = 1/\Delta f$ is given by $c * K * \log(1 + S/K)$, where c_1 is a constant, therefore,

$$F_{CS,1} = c_1 K \log(1 + S/K) \Delta f. \quad (12)$$

Compact Modeling: The number of samples needed during $T = 1/\Delta f$ is given by $c * K * \log(1 + S'/K)$, where c_2 is a constant, therefore,

$$F_{CS,2} = c_2 K \log(1 + S'/K) \Delta f. \quad (13)$$

Because $F_{Nq} = 2BW = 2S\Delta f$, the corresponding NSR for both schemes are given by:

Direct Modeling:

$$NSR_1 = \frac{F_{CS,1}}{F_{Nq}} = \frac{c_1}{2} NSP \log(1 + 1/NSP), \quad (14)$$

Compact Modeling:

$$NSR_2 = \frac{F_{CS,2}}{F_{Nq}} = \frac{c_2}{2} NSP \log(1 + 1/ESP). \quad (15)$$

Because $ESP \geq NSP$, then $NSR_2 \leq NSR_1$. In other words, the prior knowledge about the existence of the gaps can further reduce the sampling rate when PSCS is used. This sampling rate reduction can be related with the work in [16],

[17], [18]. In [16], the authors demonstrated that the number of measurements needed in compressive sensing for robust signal recovery can be reduced by including the signal's additional structural constraints in addition to the signal sparsity, which is called *model-based* compressive sensing and the signal is called *K-model sparse*. By endowing the additional constraints, the searching range for the *K-sparse* signal will be narrowed down from a union of $\binom{S}{K}$ K -dimensional subspaces to a union of l_K K -dimensional subspaces, where $l_K \leq \binom{S}{K}$. For completeness, and to connect to our approach, we state this important observation as a theorem.

Theorem 1: [17] Let \mathfrak{L}_K be the union of l_K subspaces of K -dimensions in \mathbb{R}^N . Then, for any $t > 0$ and any

$$L \geq \frac{2}{c\delta_{\mathfrak{L}_K}^2} \left(\ln(2m_K) + K \ln \frac{12}{\delta_{\mathfrak{L}_K}} + t \right), \quad (16)$$

an $L \times S$ i.i.d. sub-Gaussian random matrix has the \mathfrak{L}_K -RIP with constant $\delta_{\mathfrak{L}_K}$ with probability at least $1 - e^{-t}$. The \mathfrak{L}_K -RIP property is sufficient for robust recovery of the *K-model sparse* signal [16].

For the frequency-domain sparse signal as defined in this paper, knowing the location of frequency gaps means that the search region for the signal is narrowed down to a union of $\binom{S'}{K}$ K -dimensional subspaces. Since $\binom{S'}{K} \approx (S'/K)^K$, with the direct modeling, $l_K = \binom{S'}{K}$ and the number of measurements needed is $O(K \log(S'/K))$; and with compact modeling, $l_K = \binom{S'}{K}$ and the number of measurements needed is $O(K \log(S'/K))$.

The compact modeling can be very beneficial when the signal's ESP is not small while NSP is small. Fig. 7 shows how NSR varies with ESP for a given NSP , and Fig. 8 shows how NSR varies with NSP for a given ESP , where the solid lines are simulation results and the dashed lines are the predicted NSR according to Equation (15). When $EBW = NBW$, i.e., there is no gap or no prior knowledge of such gaps, the dotted lines give a prediction of NSR which is close to the simulation results. The constant c_2 in the equation (15) is calculated by curve matching over the simulated points. As shown, the simulation results match the prediction equation very well, where NSR is linearly proportional to NSP and logarithmically proportional to $1/ESP$. The reasoning behind this relationship can be understood from two aspects. (i) Given ESP , NSP is determined by the gaps. The traditional Nyquist sampling is the same regardless of any gaps, whereas CS can take advantage of this prior knowledge, reflected in the linear gain in NSP . (ii) Given NSP , NSR is determined by the reconstruction algorithms, which usually have a logarithmic relation.

The spectrum sensing for cognitive radio provides a very suitable scenario where we can utilize the compact modeling to reduce the compressive sampling rate, because it is possible for the sensing radio to know the locations of frequency gaps in advance. For example, if we know that the 2 GHz frequency band are heavily loaded with high probability and therefore there is a little chance that there exist spectrum holes within this band, the preselect filter of the cognitive radio receiver

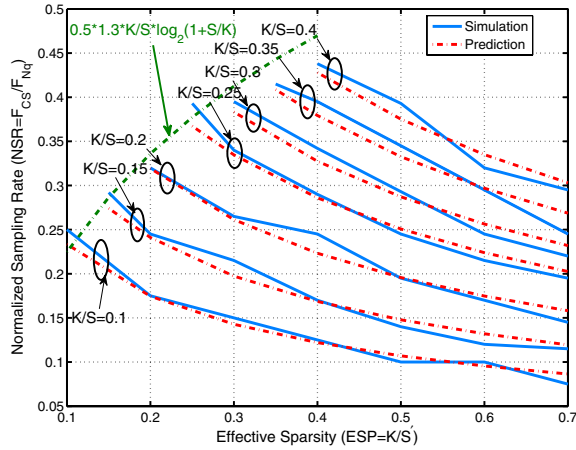


Fig. 7. Normalized Sampling Rate vs. the Effective Sparsity.

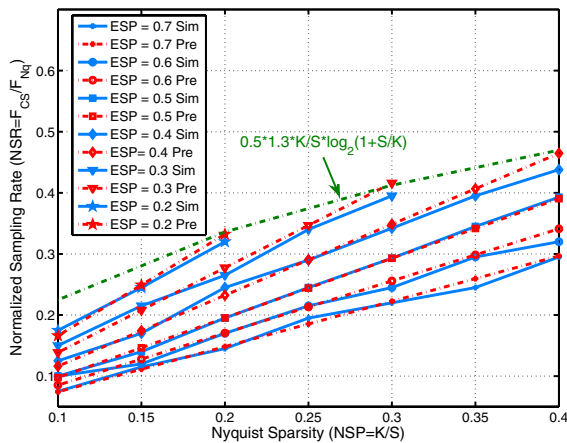


Fig. 8. Normalized Sampling Rate vs. the Nominal Sparsity.

can null out the signal within this particular band before sending the signal to the sensing radio, which results in some frequency gaps and makes the signal's $NSP < ESP$. By using the compact modeling, the sampling rate reduction will be significant when NSP is small, even if the usage of each frequency band may be high.

VI. CONCLUSIONS

Because of the difficulty in designing high-speed, high-resolution ADCs, it is very challenging to do spectrum sensing for wideband CRs, especially when the bandwidth expands from hundreds of MHz to several GHz. Fortunately, the sparsity on the current frequency usage makes it possible to use the proposed parallel compressive sensing architecture to reduce the sampling rate at the sensing radio. The mixed-signal CS avoids the necessity of a high-speed, high-resolution Nyquist rate ADC. The parallel structure brings flexibility and scalability in design, and practical wideband spectrum sensing

can be realized by carefully balancing the complexity and the sampling rate. If a priori knowledge about the signal structure is available, compact modeling can bring extra reduction in the required sampling rate. Analysis and simulation show that the proposed architecture can process the analog signal with only 10%-40% of the Nyquist sampling rate depending on the sparsity of the input analog signal.

REFERENCES

- [1] J. Mitola III, "Cognitive radio: An integrated agent architecture for software defined radio," Ph.D. dissertation, Royal Institute of Technology (KTH), May 2000.
- [2] S. Haykin, "Cognitive radio: Brain-empowered wireless communications," *IEEE J. Sel. Areas Commun.*, vol. 23, no. 2, pp. 201–220, Feb. 2005.
- [3] I. F. Akyildiz, W. Lee, M. C. Vuran, and S. Mohanty, "NeXt generation/dynamic spectrum access/cognitive radio wireless networks: A survey," *Computer Networks*, vol. 50, pp. 2127–2159, 2006.
- [4] Q. Zhao and B. M. Sadler, "A survey of dynamic spectrum access," *IEEE Signal Process. Mag.*, vol. 24, no. 3, pp. 79–89, 2007.
- [5] D. B. Cabric, "Cognitive radios: System design perspective," Ph.D. dissertation, Univ. of California at Berkeley, Dec. 2007. [Online]. Available: <http://www.eecs.berkeley.edu/~danijela/DanijelaPhDthesis.pdf>
- [6] E. A. M. Klumperink, R. Shrestha, E. Mensink, V. J. Arkesteijn, and B. Nauta, "Polyphase multipath radio circuits for dynamic spectrum access," *IEEE Commun. Mag.*, pp. 104–112, May 2007.
- [7] R. H. Walden, "Performance trends for analog-to-digital converter," *IEEE Commun. Mag.*, pp. 96–101, Feb. 1999.
- [8] D. L. Donoho, "Compressed sensing," *IEEE Trans. Inf. Theory*, vol. 52, pp. 1289–1306, Apr. 2006.
- [9] E. J. Candès, J. Romberg, and T. Tao, "Robust uncertainty principles: Exact signal reconstruction from highly incomplete frequency information," *IEEE Trans. Inf. Theory*, vol. 52, pp. 489–509, Feb. 2006.
- [10] Z. Tian and G. B. Giannakis, "Compressed sensing for wideband cognitive radio," in *IEEE ICASSP'07*, vol. 4, Apr. 2007, pp. 1357–1360.
- [11] Z. Yu, S. Hoyos, and B. M. Sadler, "Mixed-signal parallel compressed sensing and reception for cognitive radio," in *IEEE ICASSP'08*, Mar. 2008.
- [12] FCC, "Spectrum policy task force report," ET Docket, Tech. Rep. 02-135, 2002.
- [13] J. N. Laska, S. Kirolos, R. G. Baraniuk, and et al, "Theory and implementation of an analog-to-information converter using random demodulation," in *IEEE Int. Symp. on Circuits and Systems (ISCAS)*, May 2007, pp. 1959–1962.
- [14] E. J. Candès and M. B. Wakin, "An introduction to compressive sampling," *IEEE Signal Process. Mag.*, Mar. 2008.
- [15] S. Sarvotham, D. Baron, and R. Baraniuk, "Compressed sensing reconstruction via belief propagation," *Rice ECE Department Technical Report TREE 0601*, 2006.
- [16] R. G. Baraniuk, V. Cevher, M. F. Duarte, and C. Hegde, "Model-based compressive sensing," 2008, preprint. [Online]. Available: <http://www.ece.rice.edu/~duarte/images/ModelCS082008.pdf>
- [17] T. Blumensath and M. E. Davies, "Sampling theorems for signals from the union of finite-dimensional linear subspaces," *IEEE Trans. Inf. Theory*, 2008, accepted. [Online]. Available: <http://www.see.ed.ac.uk/~tblumens/papers/BDIT07.pdf>
- [18] Y. C. Eldar and M. Mishali, "Robust recovery of signals from a union of subspaces," 2008, preprint. [Online]. Available: http://arxiv.org/PS_cache/arxiv/pdf/0807/0807.4581v1.pdf